ELSEVIER

European Journal of Cancer 40 (2004) 2734–2741

European Journal of Cancer

www.ejconline.com

Molecular biomarkers and site of first recurrence after radiotherapy for head and neck cancer

Özlem U. Ataman [a,b], Søren M. Bentzen [a,*], George D. Wilson [a], Frances M. Daley [a], Paul I. Richman [c], Michele I. Saunders [d], Stanley Dische [d]

[a] *Gray Cancer Institute, Group for Human Cancer Biology and Informatics, Mount Vernon Hospital, P.O. Box 100, Northwood, Middlesex HA6 2JR, UK*

[b] *Medical School Radiation Oncology Department, Dokuz Eylül University, Izmir, Turkey*

[c] *Department of Pathology, Mount Vernon Hospital, Northwood, Middlesex, UK*

[d] *Marie Curie Research Wing, Mount Vernon Hospital, Northwood, Middlesex, UK*

Received 5 August 2004; accepted 10 August 2004
Available online 2 October 2004

Abstract

The prognostic significance of a panel of molecular biomarkers in head and neck squamous cell carcinoma (HNSCC) for first failure site (primary (T), nodal (N) or distant (M)) was analysed in 309 patients randomised to continuous hyperfractionated accelerated radiotherapy (CHART) *vs.* conventionally fractionated radiotherapy. Multivariate competing risks analysis was performed using an accelerated failure-time model. First-order interactions between each marker and trial arm were also tested. Bcl2-positivity increased the time to T- and N-failures, increasing cyclin D1 score decreased the time to N-failures. A random proliferative pattern and low Ki-67 decreased the time to M-failures. A high CD31 score was associated with a significantly longer time to T-failure after CHART, but not after conventional fractionation. Risks of T-, N- and M-failures could be estimated for individual patients. Competing risks analysis of failure sites allows the rational selection of patients for more aggressive loco-regional or systemic therapy.

Keywords: Molecular biomarkers; Competing risks; Head and neck cancer

1. Introduction

Surgery, radiation therapy and chemotherapy, all play a role in the curative management of head and neck squamous cell carcinoma (HNSCC) [1]. These modalities, alone or in combination, allow the oncologist to give varying weights to the local, regional and systemic treatment intensity. At the same time, the overall treatment intensity is limited by early and late treatment-related morbidity and this poses the challenge of optimising the combination of the three modalities, while staying within the limits of patient tolerance. Optimisation of therapy in an individual patient would ideally require a quantitative assessment of the risks of relapsing in primary, nodal or distant positions after a specific therapy.

Most studies in the literature are concerned with a specific failure site, e.g., loco-regional failure after radiation therapy, or, at the other end of the spectrum, composite outcome measures like overall or disease-free survival. Disease-free survival is of obvious interest to both the patient and the physician, but does not convey any information about the failure site and therefore does

* Corresponding author. Tel.: +44 1923 845 468; fax: +44 1923 842 870.
E-mail address: bentzen@gci.ac.uk (S.M. Bentzen).

0959-8049/$ - see front matter
doi:10.1016/j.ejca.2004.08.019

not point towards any rational change in the treatment strategy. However, studying a single failure site does not provide any information on the risk of other types of failures. Even worse, a patient with a high risk of, say, distant relapse might appear to have a low risk of loco-regional failure, simply because a distant failure would effectively prevent prolonged observation of the loco-regional tumour outcome. Technically, loco-regional and distant relapse are *competing risks*, both of them requiring prolonged observation of the patient, but when one of them occurs, this will in most cases effectively shorten the period of being at risk of failing due to the competing cause.

Statistical methods for analysing competing risks have been available since the 1970s [2,3] but have, so far, only found limited use in the analysis of outcome data after cancer therapy [4–6]. The conceptual attraction of competing risks analysis is that it takes both the type of failure and the time to failure into account and allows an estimation of failure-site-specific prognostic factors.

The aim of this study was to analyse the prognostic significance of a panel of immunohistochemical biomarkers in 309 patients in relation to specific types of failures after definitive radiation therapy in a competing risks analysis. From this analysis, an individual *risk profile* is derived in the form of individual prognostic indices for failure in primary (T), nodal (N) and distant (M) positions. Furthermore, a possible interaction is tested between these biomarkers and any clinical benefit from strongly accelerated radiotherapy that had randomly been assigned to a subset of the patients.

2. Patients and methods

2.1. Clinical study

The patients in this study were drawn from the randomised multicentre trial of continuous hyperfractionated accelerated radiotherapy (CHART) *vs.* conventional radiotherapy in head and neck cancer [7]. A total of 918 patients were included in the trial over a 5-year period in 11 centres. Patients with HNSCC in the main anatomical sub-sites of the head and neck, with the exception of T1 N0 tumours, were randomised to CHART, delivering 54 Gy in 36 fractions over 12 days, or to conventional radiotherapy, delivering 66 Gy in 33 fractions over 6.5 weeks. An uneven allocation ratio, 60:40, in favour of CHART was used. The present study includes 309 patients who had complete data on the expression of a panel of molecular markers. The clinical and pathological characteristics of this group of patients are described in Table 1. Details of the radiotherapy and the overall results of the trial have been published recently in Ref. [7].

Table 1
Clinical and pathological prognostic factors that were analysed and their covariate scores ($n = 309$)

Characteristics	Category	Score	*n*	(%)
Age	Continuous		309	(100)
Gender	Male	1	225	(72.8)
	Female	2	84	(27.2)
WHO	No restriction	1	202	(65.4)
	Restriction	2	107	(34.6)
Treatment arm	CHART	1	184	(59.5)
	Conventional	2	125	(40.5)
T stage	T1	1	9	(2.9)
	T2	2	137	(44.3)
	T3	3	103	(33.3)
	T4	4	60	(19.4)
N stage	N0	1	188	(60.8)
	N+	2	121	(39.2)
Histology	Well differentiated	1	66	(21.4)
	Moderately differentiated	2	145	(46.9)
	Poorly differentiated	3	61	(19.7)
	Squamous, Not specified	4	37	(12.0)
Site[a]	Oropharynx	1	82	(26.5)
	Hypopharynx	2	34	(11.0)
	Larynx	3	138	(44.7)
	Oral cavity	4	42	(13.6)
Ki-67	<20%	1	144	(46.6)
	20% or more	2	165	(53.4)
Proliferative pattern	Marginal	1	52	(16.8)
	Intermediate	2	104	(33.7)
	Mixed	3	42	(13.6)
	Random	4	111	(35.9)
p53 score	Negative	1	156	(50.5)
	Sporadic	2	77	(24.9)
	Positive	3	76	(24.6)
p53 intensity	Weak	1	177	(57.3)
	Intermediate	2	54	(17.5)
	Strong	3	78	(25.2)
CD31 score	Low	1	125	(40.5)
	Intermediate + strong	2	184	(59.5)
bcl-2 score	Negative	1	269	(87.1)
	Positive	2	40	(12.9)
Cyclin D1	Continuous		309	(100)

WHO performance status, World Health Organization; CHART, continuous hyperfractionated accelerated radiotherapy.

[a] 13 tumours (4%) originated in other sites within the head and neck.

2.2. Histological material

Histological material was obtained, retrospectively, from the referring hospitals. Each pathology department was requested to either provide the original blocks for processing at Mount Vernon Hospital or to cut up to twelve 4 μm sections mounted onto poly-L-lysine-coated slides. Each specimen was examined by a pathologist in order to confirm the presence of assessable SCC tumour.

2.3. Immunohistochemical staining

Sections were dried overnight at 37 °C. Prior to antibody staining, the slides, for each marker, were blocked for endogenous peroxidase activity with a 3% solution of hydrogen peroxide in methanol for 30 min. Microwave irradiation was used to unmask the binding epitopes using either 10 mM citric acid (pH 6.0) for Ki-67, p53, bcl-2 and CD31 or 1 mM ethylene diamine tetra acetic acid (EDTA) (pH 8.0) in the case of cyclin D1. A cycle of 3 five-minute irradiations was used for all antibodies except bcl-2, which required only two cycles. The slides were then left to stand for 10 min in buffer at room temperature before being washed thoroughly in tap water. After three washes in Tris-buffered saline (TBS), the slides were incubated in the different antibodies in TBS containing 1 drop per ml of Dako Serum Free Protein block (Dako Ltd, High Wycombe, X0909) for 1 h at room temperature. The monoclonal antibodies to p53 (clone DO-7, Dako Ltd.) was used at a 1:75 dilution, CD31 (PECAM-1, Dako Ltd.) at 1:30, bcl-2 (clone 124, Dako Ltd.) at 1:40 and cyclin D1 (Novacastra, Peterburgh, clone NCL-Cyclin D1-GM) at a dilution of 1:75. The antibody against Ki-67 was a rabbit polyclonal (clone MIB-1, Dako Ltd.) and was used at 1:75 dilution. After three further washes in TBS, biotinylated rabbit anti-mouse antibody (Dako Ltd E0354) or, in the case of Ki-67, biotinylated swine anti-rabbit antibody (Dako Ltd.) diluted 1:400 in TBS was applied for 1 h at room temperature. After three further washes, ABC complex (Dako Ltd K0355) was added for 1 h at room temperature. The staining was visualised by adding diaminobenzidine (Vector Labs. DAB kit SK 4100) for 5 min at room temperature. Cyclin D1 was stained at a later date and the Dako Envision polymer kit (Dako Ltd., K4006) was added for 30 min. Following three further washes in TBS, Envision DAB (Dako Lt.d) was added for 5 min. All slides were washed well in tap water and counterstained with Mayers Haematoxylin for 10 s – 1 min and then dehydrated, cleared and mounted in DPX.

2.4. Assessment of staining

All slides were inspected for the presence of assessable tumour and semi-quantitatively analysed by a consultant pathologist, except in the case of cyclin D1 staining.

For Ki-67, the slides were visually scanned and ascribed to one of two scores; 1 = less than 20% positive cells, 2 = 20% or more positive cells. In addition, the proliferation pattern was assessed as previously described in Ref. [8], where 1 = marginal (most organised), 2 = intermediate (mainly organised), 3 = mixed (more than one pattern usually including random) and 4 = random (diffuse, disorganised staining). Slides stained for bcl-2 were scored as negative if less than 5% of cells were stained and positive otherwise. p53 was classified as 1 = negative (less than 5% positive cells), 2 = sporadic (5–75% cells positive) and 3 = all (>75% positive cells). The vessel count identified by CD31 staining was classified in 10 high-power fields as 1 = up to 35 vessels, 2 = 35–55 vessels and 3 = greater than 55 vessels. Cyclin D1 was assessed by manual counting aided by an in-house image acquisition system incorporating a CCIR-format 3-CCD chip colour camera coupled to a PC-based video-rate frame grabber. Software routines for image acquisition, normalisation and storage have been developed as have grids and manual counting data recording. At least 10 high-power fields (40× objective) were counted for each specimen.

2.5. Endpoints and statistical analysis

All patients were seen weekly for the first 6 weeks from the start of the treatment. Further follow-ups were at 8 weeks and 3 months after the first day of treatment, subsequently 3 monthly to 2 years, 6 monthly to 5 years and annually thereafter.

Local and nodal failures were recorded at the time when clinically definitive tumour growth was detected in the primary site or in the nodes. Distant failure was defined as appearance of metastatic disease outside of the irradiated volume.

In each patient, the time to first failure and its location were recorded. Patients without clinical progression were censored at the time of their last follow-up. In the competing risks method used here, the failure types considered need to be mutually exclusive. Nine patients with isolated distant failures as the first failure and 11 patients failing distantly with synchronous loco-regional failures were classified as having failed in M-position. Six patients with isolated nodal failure and 35 patients with synchronous nodal and local failure were classified as having failed in N-position. Patients with isolated failures in the primary site were classified as having failed in T-position. All event times were calculated from the first day of radiotherapy.

Competing risks analysis was performed using the Dynamic 7, PC version of the Biomedical Data Package (BMDP) [9]. An accelerated failure-time model with a log–logistic hazard function was used to assess the effects of covariates on the time to first failure and its site for the whole patient group. The BMDP competing risks analysis estimates failure-site-specific regression coefficients and standard errors of the estimate (SEE) for each covariate. A positive regression coefficient means that increasing values of the covariate score will *increase* the time to failure, whereas a negative regression coefficient means that increasing values of the covariate will *decrease* the time to failure.

All available prognostic factors, age, gender, World Health Organization (WHO) performance status, treatment, T stage, N stage, histological grade, site, Ki-67, p53, CD31, bcl-2, cyclin D1 scores and proliferative pattern, were assigned numerical scores as shown in Table 1 and entered into the model. Non-significant variables ($P > 0.05$), i.e., variables with no significant influence on time to failure and/or site of failure, were excluded from the model in a stepwise manner. In the reduced model, interaction terms between the trial arm and each molecular marker were included one by one. If the interaction term was more statistically significant than the term representing the marker itself, the interaction term was retained in the model.

From the regression coefficients of covariates in the final model, prognostic indices for each of the three failure types were calculated for each individual patient. For each failure type, the corresponding prognostic index, together with the site-specific underlying log-logistic failure time distribution, allows estimation of the 2-year failure rate as described in our previous study in Ref. [6]. For each failure type, three prognostic groups were defined according to the 33-percentiles of the 2-year failure rate estimates.

Modelled failure time distributions were visually compared with Kaplan–Meier estimates over time to examine the goodness-of-fit of the model.

All P-values are from 2-tailed tests.

3. Results

Isolated local failure, T-failure, was the first failure in 99 patients and nodal failure with or without local failure, N-failure, was the first failure in 41 patients. Twenty patients experienced an M-failure as their first failure, i.e., they had a distant failure with or without a synchronous loco-regional failure. The number of censored patients was 149.

Stepwise regression was conducted as described above. The final reduced model included 7 variables: T and N stage, proliferative pattern, bcl-2, cyclin D1, Ki-67 and the interaction term: treatment-arm × CD31 score. Table 2 shows the regression coefficients for T-, N- and M-failures together with their standard errors. Fig. 1 shows these estimates with 95% Confidence Limits for the 7 covariates included in the final model. If, for a given type of failure, the 95% Confidence Limits for the regression coefficient do not overlap zero, the coefficient has a statistically significant influence on the time to that type of failure. A positive regression coefficient corresponds to an increasing time to failure with increasing scores of the covariate and *vice versa* for a negative coefficient.

Patients with higher Cyclin D1 scores had significantly decreased times to N-failure (Fig. 1), whereas this covariate had no significant effect on time to T- and M-failures. Node-positive patients at the time of diagnosis had decreased time to N-failure, as expected. Increasing T stage was associated with a shorter time to both T- and M-failures. Higher Ki-67 scores (>20%) were associated with an increased time to M-failure, without any significant effect on T- and N-failures (Fig. 1). Bcl-2-positivity was associated with an increased time to T- and N-failures, i.e., it was a favourable prognostic marker (Fig. 1).

Among the first-order interactions with therapy, only CD31 score was statistically significant ($P = 0.02$), with a regression coefficient showing an increased benefit of CHART relative to conventional fractionation in patients with a high CD31 score.

In order to explore this association further, we looked at the association between vascularity and histopathological grade of differentiation in the database. In 345 patients, who had a CD31 score as well as a histopathological grading, increasing values of the CD31 score was associated with more differentiated tumours (Kendall's τ, $P = 0.009$).

3.1. Individual risk profiling

From the regression coefficients of each covariate, prognostic indices for T-, N- and M-failures were calculated for each individual patient. These again facilitated

Table 2
Failure-specific covariate coefficients with standard errors in the final model

Covariate	Local failure (T)		Nodal failure (N)		Distant failure (M)	
	Coefficient	SEE	Coefficient	SEE	Coefficient	SEE
P. pattern	−0.13	0.15	−0.23	0.24	−0.77	0.30
Cyclin D1	−0.007	0.005	−0.02	0.008	0.001	0.01
Ki-67	0.42	0.34	0.42	0.51	1.53	0.64
N stage	0.24	0.33	−3.06	0.64	−0.86	0.58
Bcl-2	1.36	0.51	2.08	0.89	0.22	0.70
TRT*CD31	0.40	0.17	−0.14	0.27	0.40	0.32
T stage	−0.76	0.19	0.05	0.30	−1.33	0.40

SEE, standard errors of the estimate; P pattern, proliferative pattern; TRT* CD31, treatment-arm X CD31 score.

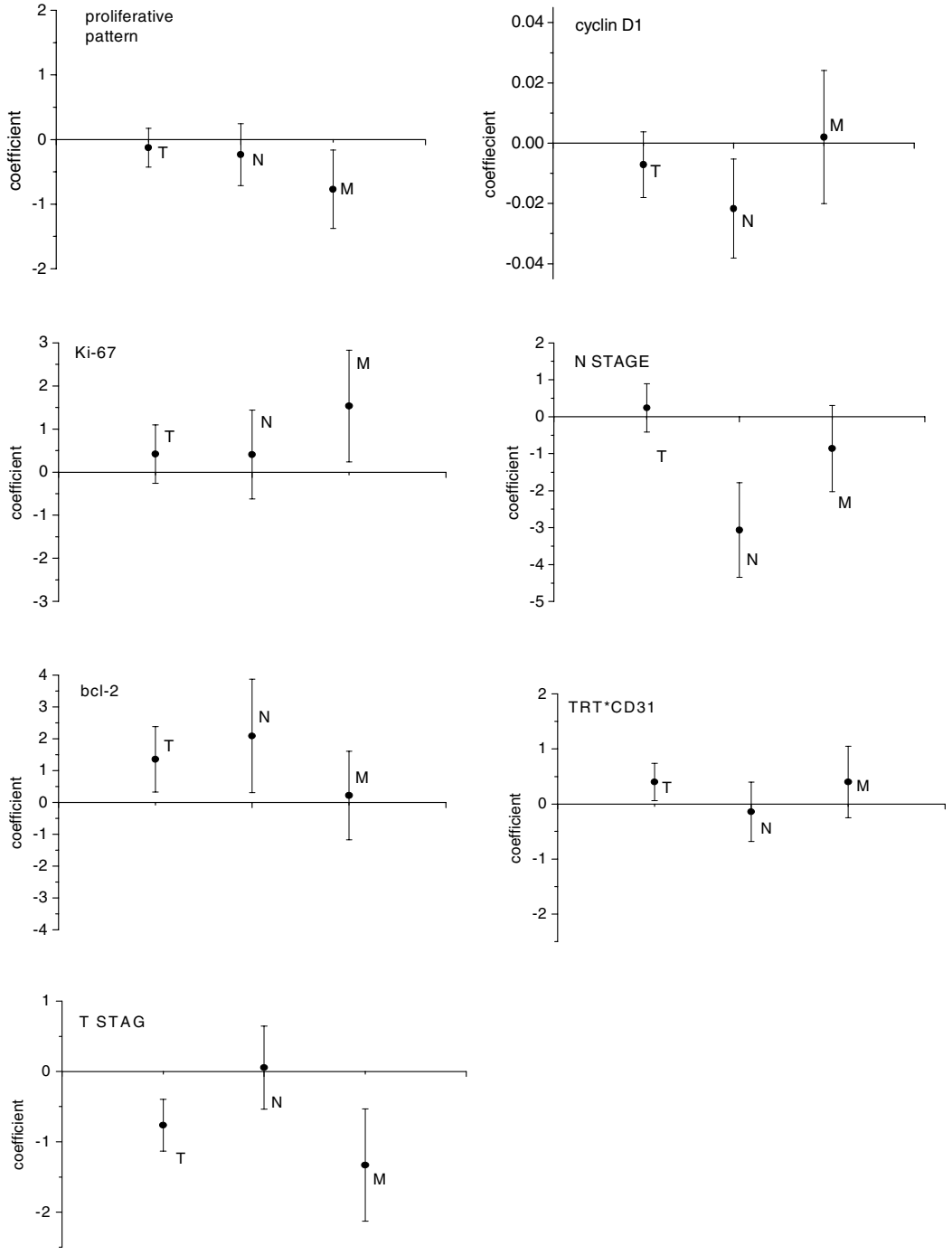

Fig. 1. Regression coefficients with 95% Confidence Limits for distant (M), nodal (N) and local (L) failure for the 7 covariates in the final model. Positive (negative) values correspond to a prolonged (shorter) time to the relevant type of recurrence with increasing values of the covariate.

estimation of 2-year rates for each failure type. Fig. 2 shows a pseudo-3-dimensional (3D) graph of the estimated 2-year failure rates in 10 selected cases. The number of cases plotted was limited for graphical clarity and the ten cases were selected to give an impression of the variation in the failure rates. The 33-percentiles of the 2-year failure estimates were used to define 3 prognostic groups for each type of failure with different risks of T-, N- and M-failure. For each failure type, failure rates were highly significantly different ($P < 0.00001$, log-rank test). Modelled failure-time distributions were compared graphically with Kaplan–Meier estimates over time in order to check the model fit (Figs. 3–5) and for each failure type, this appeared to be very good.

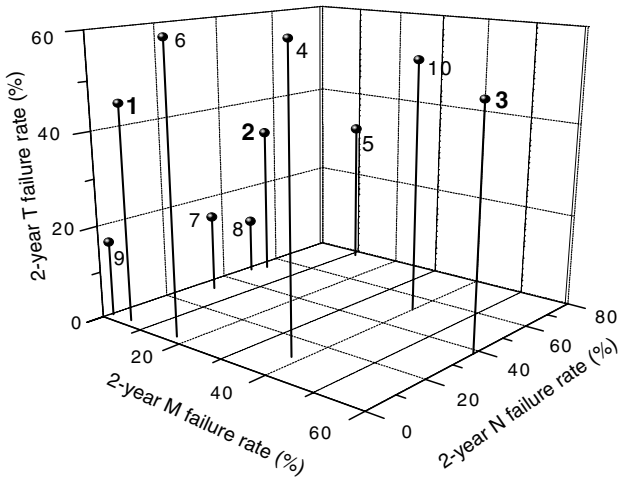

Fig. 2. Scatter plot of the estimated T, N and M 2-year failure rates for ten selected patients. Each sphere represents a single patient and the drop lines show their projection on the M-, N-failure plane.

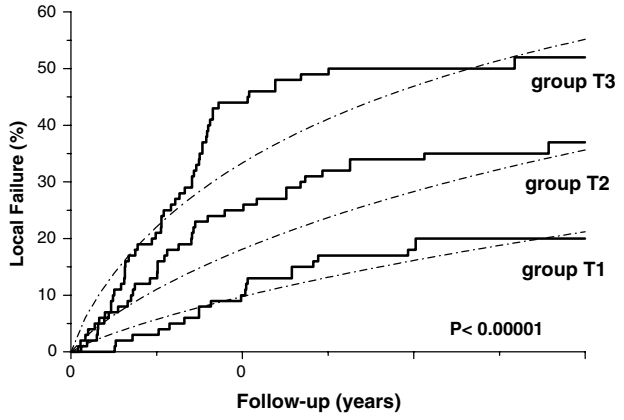

Fig. 3. Modelled local-failure rates over time in low-, intermediate- and high-risk patients compared with 1-KM estimates (full lines).

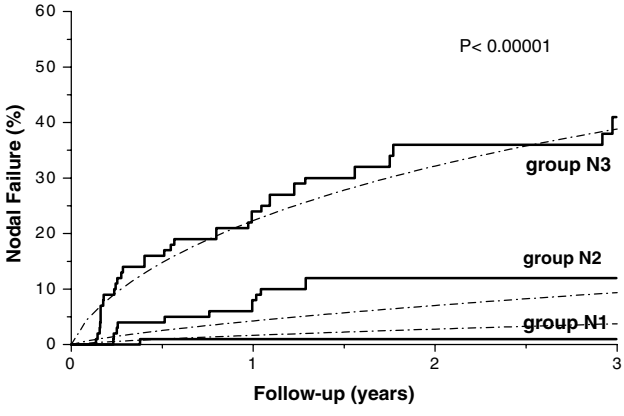

Fig. 4. Modelled nodal-failure rates over time in low-, intermediate- and high-risk patients compared with 1-KM estimates (full lines).

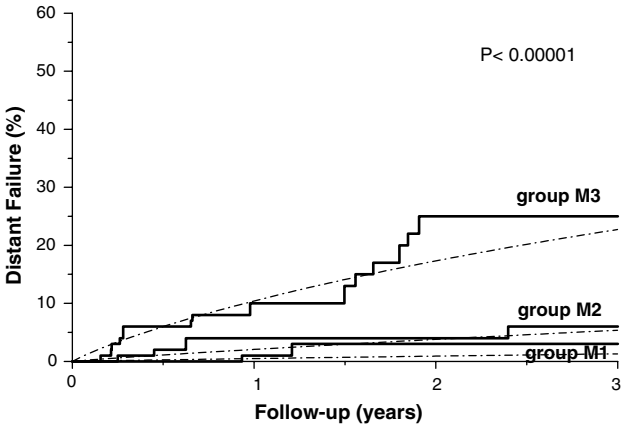

Fig. 5. Modelled distant-failure rates over time in low-, intermediate- and high-risk patients compared with 1-KM estimates (full lines).

4. Discussion

Optimising loco-regional control, disease-free and overall survival remains a challenging goal in the management of locally advanced HNSCC. Although significant therapeutic gains from altered fractionation and combined chemoradiation have been demonstrated in a number of randomised controlled trials, therapeutic outcome is far from satisfactory, with relatively high loco-regional failure rates of around 50% after 3 years and an overall 5-year survival rate of 50% [1,10]. As these intensified therapies tend to be associated with increased toxicity, selection of subgroups of patients who would benefit from a specific treatment schedule could potentially improve the overall therapeutic efficacy.

Disease-free survival is a composite endpoint, where an 'event' is any recurrence (local, regional or distant) or death from any cause, whichever comes first [11]. This endpoint does not provide information on the location of the first failures and therefore is less useful in pointing towards specific therapeutic management strategies. It is also conceivable that various molecular tumour markers may have a differential effect on the risk of specific types of failure and this may lead to a loss of statistical power – as well as a loss of information – in analyses using disease-free survival or cause-specific survival as the endpoint. We therefore decided to apply a biostatistical method, known as competing risks analysis, that has been developed for multivariate analysis of factors influencing the type of and time to first failure [2,3].

Advances in the understanding of the molecular mechanisms of tumour development and disease progression has been the stimulus for many studies seeking to identify a relationship between various biomarkers and the risk for recurrence of the disease or selecting patients for more aggressive therapy or alternative treatment modalities [12]. This is the first report of the potential of utilising multiple molecular markers to de-

rive prognostic indices for each type of failure using competing risks analysis in a large cohort of uniformly-treated patients in HNSCC. The markers had been chosen to reflect different biological processes that might be involved in the response to treatment mainly proliferation (Ki-67), cell cycle deregulation (p53 and cyclin D1), apoptosis (bcl-2) and vascularity (CD31). Except for p53, all other molecular biomarkers in this study were predictive for at least one of the types of failures. The regression coefficients in the final model and their relation to T-, N- and M-position failures were plotted in Fig. 1, which gives a simple overview of whether a variable has a positive or negative effect on the time from therapy to the occurrence of a specific type of failure and whether this influence is significant or not. The data presented in Table 2 and Fig. 1 show both expected and unexpected associations of the factors with local, nodal and distant failure. As expected, increasing T stage was associated with a decreasing time to both local and distant failure, but without effect on nodal failure, whilst increasing N stage predicted strongly both nodal and distant failure, but not isolated local relapse. Amongst the biological parameters, loss of proliferative organisation, as indicated by the proliferation pattern, was associated with a significantly shorter time to distant failure. Paradoxically, increased proliferation rate (Ki-67 >20%) was predictive of an increased period to metastasis. This observation may seem at odds with the generally held view that increased proliferation is linked to increased biological aggressiveness, but it may instead reflect an enhanced response to treatment. Increasing cyclin D1 was associated with a higher propensity for both local and, in particular, nodal failure; this is in agreement with reports in the literature [13]. bcl-2, as we have previously shown [14], predicts for both longer local control and loco-regional control times.

Using this approach, selection of primary therapeutic interventions could be based on the consideration of the contribution of relative risks of failures at local (T), nodal (N) and distant (M)-positions. For example, prediction of the precise local failure rate for an individual patient at the time of presentation would provide the possibility to intensify local treatment or select ideal patients for organ preservation, thus avoiding the need for salvage surgery. Patient one in Fig. 2 exemplifies this, where the estimated 2-year T-, N- and M-failure rates were 46%, 0.5% and 0.3%, respectively. This patient could be a candidate for intensified local treatment, small volume, high-dose, altered fractionation schedule or intensity-modulated radiotherapy (IMRT) depending on the site of origin. Patient two (Fig. 2) could be considered for intensified loco-regional treatment possibly requiring elective neck dissection due to a higher risk of both local (33%) and nodal (53%) failure, but very low M-failure (2%) risk. However, for patient three (Fig. 2), the estimated 2-year M-failure rate was 56%, much higher than the other types of failures, and for this patient adjuvant chemotherapy would be indicated in addition to radiotherapy.

These individual estimates were grouped together (in Figs. 3–5) using the 33-percentiles of the 2-year failure rates to define different prognostic groups. Estimated local failure rates at 3 years were 20%, 37% and 51% for groups T1, T2 and T3, respectively. The differences between groups were more pronounced for N- and M-failures. A patient in group N3 would have a nodal failure rate of 40%, compared with a patient with 10% failure rate in group N2 and 2% in group N1. In group M3, the distant failure rate was 27%. The comparisons produced a log-rank P value of $P < 0.00001$ in all cases.

Overall, the CHART trial found no significant difference in loco-regional tumour control between the two arms of the trial [7]. This has been thought to reflect that a sub-population of tumours might have had a disadvantage from the relatively low absorbed dose, whereas others had an advantage following the very short, intensive radiotherapy schedule. Another concern has been that the 12-day CHART schedule might not have given sufficient time for re-oxygenation causing potential problems in the control of hypoxic tumours. All of this has stimulated interest in the identification of clinical or tumour characteristics that would be predictive for a benefit from CHART relative to conventional therapy. In the present analysis, a significant interaction was seen between randomisation to CHART and the vascularity, with increasing CD31 scores being associated with a benefit from CHART. This raises two interesting speculations: the well-vascularised tumours may be less affected by the possible reduced re-oxygenation during the CHART regimen or it may be that these are the tumours where a proliferative response to the radiotherapy trauma can be most effectively activated. A previous report [15] suggested that well-differentiated tumours may have a more pronounced treatment-time dependency. It is possible that differentiation is only an epi-marker for an underlying biological characteristic of the tumour and in this study we actually found a significant association between histopathological grade and CD31 score. Thus, the effect seen here is consistent with the findings by Hansen and colleagues [15] but histopathological grade in itself was not of prognostic importance in our study.

In summary, multivariate analysis using competing risks models, as explored in this paper, has three potential fields of application in exploring the clinical significance of new biological markers, stratification of patients into trials of new treatments and for tailoring of therapy based on individual risk profiling. With the current move towards more indications for combined loco-regional and systemic therapies, studies of failure-type specific predictive markers are of great interest

and we feel that the approach taken here warrants further study.

Conflict of Interest Statement

None declared.

Acknowledgements

This research was funded by the Scott of Yews Trust and the Gray Laboratory Cancer Research Trust and by the Radiation Oncology Department of the Dokuz Eylul University Medical School. We wish to acknowledge the great efforts of all members of the CHART Steering Committee: A. Barrett (Chairman), D. Coyle, B. Cottier, A.M. Crellin, P. Dawes, S. Dische, M.F. Drummond, C. Gaffney, D. Gibson, A. Harvey, J.M. Henk, T. Herrmann, B. Littbrand, J. Lttler, F. Macbeth, D.A.L. Morgan, H. Newman, M.K.B. Parmar, A.G. Robertson, M. Robinson, R.I. Rothwell, M.I. Saunders, R.P. Symonds, J.S. Tobias, M.J. Whipp, H. Yosef.

References

1. Bernier J, Bentzen SM. Altered fractionation and combined radiochemotherapy approaches: pioneering new opportunities in head and neck oncology. *Eur J Cancer* 2003, **39**, 560–571.
2. Lagakos SW. A covariate model for partially censored data subject to competing causes of failure. *Appl Statist* 1978, **27**, 235–241.
3. Kalbfleisch JD, Prentice RL. *The statistical analysis of failure time data*. New York, NY, Wiley, 1980., p. 21–38.
4. Arriagada R, Kramar A, Le Chevalier T, De Cremoux H. Competing events determining relapse-free survival in limited small-cell lung carcinoma. The French Cancer Centers' Lung Group. *J Clin Oncol* 1992, **10**, 447–451.
5. Chapman JW, Fish EB, Link MA. Competing risks analyses for recurrence from primary breast cancer. *Br J Cancer* 1999, **79**, 1508–1513.
6. Ataman ÖU, Bentzen SM, Saunders MI, Dische S. Failure-specific prognostic factors after continuous hyperfractionated accelerated radiotherapy (CHART) or conventional radiotherapy in locally advanced non-small-cell lung cancer: a competing risks analysis. *Br J Cancer* 2001, **85**, 1113–1118.
7. Dische S, Saunders M, Barrett A, Harvey A, Gibson D, Parmar M. A randomized multicentre trial of CHART *versus* conventional radiotherapy in head and neck cancer. *Radiother Oncol* 1997, **44**, 123–136.
8. Bennett MH, Wilson GD, Dische S, Saunders MI, Martindale CA, *et al*. Tumour proliferation assessed by combined histological and flow cytometric analysis: implications for therapy in squamous cell carcinoma in the head and neck. *Br J Cancer* 1992, **65**, 870–878.
9. BMDP Statistical Software, PC Dynamic 7.0 1992.
10. Smith BD, Haffty BG. Molecular markers as prognostic factors for local recurrence and radioresistance in head and neck squamous cell carcinoma. *Radiat Oncol Invest* 1999, **7**, 125–144.
11. Bentzen SM. Towards evidence based radiation oncology: improving the design, analysis, and reporting of clinical outcome studies in radiotherapy. *Radiother Oncol* 1998, **46**, 5–18.
12. Anastasios NS, Cullen KJ. Molecular markers predictive of response and prognosis in the patient with advanced squamous cell carcinoma of the head and neck: evolution of a model beyond TNM staging. *Curr Opin Oncol* 2000, **12**, 229–239.
13. Michalides RJAM, van Veelen N, Hart A, Loftus B, Wientjens E, Balm A. Overexpression of cyclin D1 correlates with recurrence in a group of forty-seven operable squamous cell carcinomas of the head and neck. *Cancer Res* 1995, **55**, 975–978.
14. Wilson GD, Saunders MI, Dische S, Richman PI, Daley FM, Bentzen SM. bcl-2 expression in head and neck cancer: an enigmatic prognostic marker. *Int J Radiat Oncol Biol Phys* 2001, **49**, 435–441.
15. Hansen O, Overgaard J, Hansen HS, Overgaard M, Hoyer M, *et al*. Importance of overall treatment time for the outcome of radiotherapy of advanced head and neck carcinoma: dependency on tumor differentiation. *Radiother Oncol* 1997, **43**, 47–51.